Vibrational and thermodynamic properties of metal clusters with up to 150 atoms calculated by the embedded-atom method

Valeri G. Grigoryan* and Michael Springborg†

Physical and Theoretical Chemistry, University of Saarland, D-66123 Saarbrücken, Germany

(Received 20 July 2010; revised manuscript received 21 February 2011; published 7 April 2011)

The full vibrational spectrum of Ni_N and Cu_N clusters for clusters with N from 2 to 150 has been determined. The vibrational frequencies show a highly irregular behavior as function of cluster size and geometry. Furthermore, using the obtained results, we determine quantum mechanically the thermodynamics of the clusters using the superposition approximation. The obtained heat capacity shows clear cluster-size effects. In addition, the solid-solid transition temperature for several structural changes in nickel and copper clusters has been calculated.

DOI: 10.1103/PhysRevB.83.155413 PACS number(s): 63.22.Kn, 61.46.−w, 64.70.Nd

Clusters, of central importance to nanotechnology, are interesting materials, both from the point of view of basic research and from an application point of view. A vital issue is how the structure of a cluster depends on its size, because any property is a function of the cluster structure. Unfortunately, experimental studies do not provide this information unambiguously, nor is global-geometry optimization using *ab initio* approaches possible for clusters with more than some 10–20 atoms. Thus, the most promising approach is to use approximate, theoretical methods, as long as it is verified that they combine computational simplicity with sufficient accuracy.

In this context a very useful approach for the study of transition-metal clusters is the embedded-atom method (EAM) that was developed by Daw, Baskes, and Foiles[1–4] and is valid for metals with only little directional bonding. The scheme incorporates many-particle effects and is computationally as efficient as pair potentials. The EAM has been successfully applied to many bulk and low-symmetric problems in transition metals (see, e.g., Ref. 4). Another version of the EAM by Voter and Chen[5,6] also considers diatomic data as well as bulk properties in the fitting procedure. Moreover, the EAM is closely related (mathematically equivalent) to many other parametrized many-body models as the effective-medium theory, the glue model of Ercolessi, the Finnis-Sinclair potential, and the many-body Gupta potential.[4]

According to the EAM, the total energy of a system relative to that of the isolated atoms is given through

$$E_{\mathrm{tot}} = \sum_n F_n\left(\rho_n^h\right) + \frac{1}{2}\sum_{n,m(n\neq m)} \varphi_{nm}(R_{nm}). \qquad (1)$$

Here, ρ_n^h is the local electron density at site n, F_n is the embedding energy, and φ_{nm} is a short-range potential between atoms n and m separated by the distance R_{nm}. Different many-body approaches listed in the preceding paragraph use the same form of Eq. (1) with only different F and φ.[4] With this, it has become possible to calculate analytically the first (force vector) and second (force-constant tensor) derivatives with respect to the atomic coordinates.[2,7,8] This, in turn, has enabled us to develop high-speed computer programs to perform global structure optimization for isolated Ni_N and Cu_N clusters with N up to 150 (Refs. 9, 10) using our own Aufbau/Abbau algorithm.[11,12] We could also demonstrate that the obtained structures were in good agreement with available experimental and theoretical information. It was also checked that the two different versions of the EAM give very similar results.[13]

It is the purpose of the present contribution to extend those studies with the determination of the vibrational properties of the clusters. We thereby present a general scheme for extracting temperature-dependent properties from studies of the ground-state properties at $T = 0$ and subsequently apply it to the Ni and Cu clusters.

A knowledge of the vibrational spectrum is very important for the understanding of different properties of a cluster. They are needed for the determination of the thermodynamic properties, which in turn determine finite-temperature effects like the stability, solid-solid structural transitions, and melting of clusters.[14,15] With vibrations one could compute electron-vibration interaction in clusters and correspondingly study scattering and kinetic effects in nanocluster devices, which, however, is beyond the scope of the present work. Furthermore, vibrational modes are fingerprints of the cluster structure and, correspondingly, of the bonding between cluster atoms. Therefore, vibrational spectroscopy could be a very powerful tool for the analysis of cluster structure. The vibrational spectra of nickel clusters with $N = 2$–14, 19, 20, and 55 were calculated using a many-body Gupta potential in a study.[16] Solov'yov *et al.*[17] determined the normal vibration frequencies of small sodium clusters with $N \leqslant 20$ using the B3LYP method and obtained qualitative agreement with the predictions based on the jellium model. Very recent progress in experimental techniques[18] allowed unique infrared absorption spectra to be obtained for small isolated clusters in the gas phase via infrared multiple photon dissociation spectroscopy. Using this method in combination with theory, the geometric cluster structures of small vanadium clusters in the size range from 6 to 23 atoms were identified.[18] Using the Green's function technique and the EAM to model the atom-atom interactions, the authors of Ref. 19 presented a systematic examination of the effect of changing elemental composition on the local structure (bond lengths), vibrational density of states, and thermodynamics of the bimetallic cluster Ag_nCu_{34-n}. Furthermore, vibrations in larger low-dimensional systems, such as nanoparticles, nanocrystallines, and nanostructured surfaces, have been intensively studied theoretically[20–28] using different model potentials (EAM, effective-medium theory,

glue, Sutton-Chen, tight-binding second-moment, empirical atomistic force models, and Lennard-Jones) and techniques (slab method, Green's function approach, diagonalization of the dynamical matrix, and molecular-dynamics simulations). For those systems a low- and high-frequency enhancement of the vibrational density of states as compared to the bulk materials has been found. Experimental measurements[27,29–33] have supported these findings. Similar enhancements have been observed in computer simulations.[34,35]

Experimental studies of the melting of free sodium clusters have demonstrated that thermodynamic properties of clusters depend nontrivially on the cluster size.[36–38] Specifically, it was found that the melting temperatures are about 30% lower than the bulk value, that they show strong size-dependent effects in that one additional atom can change the melting temperature by ± 10 K, and that the geometric structures of the clusters are crucial for the melting properties. Other experiments of the thermodynamic properties of clusters[39,40] showed that small tin and gallium clusters have higher melting temperatures than the bulk. Despite much theoretical effort, a general understanding of those phenomena is still lacking.[41] Since melting is connected both to the structure and to the dynamics of the atomic lattice, a knowledge of the cluster ground-state configuration and the structures of a set of isomers (in some cases this number may be large) in combination with the full vibrational spectrum of the isomers is essential for an understanding.

Using the global-minima structures obtained before,[9,10] we determine the full vibrational spectrum of nickel and copper clusters with N up to 150 atoms. Furthermore, using those structures we determine the free energy, the entropy, the inner energy, and the heat capacity of the clusters as functions of their size. Finally, the solid-solid transition temperature T_{ss} for some structural changes in nickel and copper clusters is presented as well.

The vibrational spectrum was calculated by using the harmonic approximation, i.e., from the eigenvalues of the $3N \times 3N$ dynamical matrix $D_{ni;mj} = M^{-1}(\partial^2 E_{\rm tot}/\partial R_{ni}\partial R_{mj})$, where M is the atomic mass and R_{ni} is the ith (i.e., x, y, or z) coordinate of atom n. The harmonic approximation is good[41] in most cases and often even up to melting temperatures. The full vibrational spectrum of nickel and copper clusters was calculated for each cluster size ranging from 2 to 150 atoms. For the dimers, we found frequencies of 412 and 292 $\rm cm^{-1}$ for nickel and copper, respectively, in good agreement with experimental spectroscopic values[42,43] of 381 (Ni) and 266 $\rm cm^{-1}$ (Cu).

The size dependencies of the frequencies are not simple and cannot be described by scaling laws, but the general trend is qualitatively similar for nickel and copper clusters. Figure 1 shows the largest, lowest, and (geometrical) averaged frequencies of $\rm Ni_N$ and $\rm Cu_N$ for each cluster size in comparison with the maximum phonon frequency in the bulk. The largest frequency possesses strong oscillations. Thus, for N less than approximately 40, the strong oscillations are related partly to radical changes of the structure (e.g., a transition from the icosahedral geometry to the fcc one), but even for smaller structural changes the addition of a single atom can change this frequency markedly. For larger N only significant structural changes lead to the strong oscillations in the highest vibrational

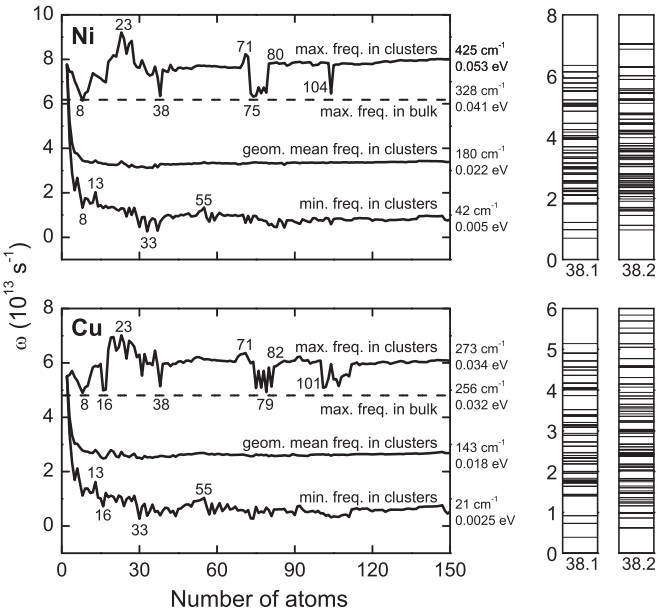

FIG. 1. The maximum, minimum, and geometric mean normal-mode frequencies of the nickel (top left) and copper (bottom left) clusters as functions of cluster size. The horizontal dashed lines in both left-hand graphs display the maximum phonon frequency in bulk. The full vibrational spectrum of the two lowest-energy structures of $\rm Ni_{38}$ (top right, narrow panels) and $\rm Cu_{38}$ (bottom right, narrow panels). The numbers to the right of the left-hand graphs display the normal frequencies at $N = 150$ in different units.

frequencies. Furthermore, the maximum frequency is lower in clusters with a structure resembling the fcc structure of the crystal (i.e., $\rm Ni_{38}$, $\rm Cu_{38}$, $\rm Cu_{79}$) as well as in clusters with decahedral motifs [around $N = 75$ (Ni, Cu), $N = 101$–103 (Cu), and $N = 104$ (Ni)] and higher in the icosahedral ones. The overall largest values of the maximum frequency are found for $17 < N < 28$ with the global maximum at $N = 23$ (whose structure is a triple icosahedron) for both nickel and copper clusters. The global-maximum values are 45–50% larger than those in bulk. All the structures for $N = 17 - 28$ possess polyicosahedral packing.[9,10] On the average, the maximum vibrational frequency in the nickel and copper icosahedral clusters exceeds that in bulk by 25–30%.

The special features of the maximum frequency plots of Fig. 1, discussed above, can be qualitatively understood from structural considerations. The energy of the higher-frequency modes is mostly defined by the local strains in the surroundings of an oscillating atom. On the other hand, a Mackay icosahedron can be obtained from 20 tetrahedra sharing a common vertex. The tetrahedra have to be distorted to be able to fill out the entire volume of the icosahedron. Thus, an icosahedron is a highly strained structure. Even more strained structures possess polyicosahedra composed of interpenetrated icosahedra. In turn, a decahedron can be constructed out of five tetrahedra sharing a common edge. To close the gap between two connecting surfaces, they have to be distorted. As a result, one obtains a perfect decahedron with internal strains which are less than in an icosahedron. There are no internal strains in fcc clusters that involve

almost (see later) nondeformed tetrahedra. Therefore, the restoring forces acting on vibrating atoms in icosahedral or polyicosahedral structures are larger. The latter respectively leads to the larger normal frequencies according to the present study. In addition it should be mentioned that the tetrahedra in fcc clusters are slightly deformed compared with those in bulk due to the contraction effect—the average bond length in metal clusters is slightly less than that in the bulk (see, e.g., Refs. 9, 10). That leads in turn to small internal strains even in fcc clusters and respectively to larger restoring forces and larger maximum frequencies in fcc clusters as compared with the bulk. As shown in Fig. 1, this effect is slightly stronger for fcc copper clusters. A similar effect of an enhancement of the high-frequency modes and the appearance of modes above the top of the bulk band also was found in nanostructured surfaces and nanoparticles.[20,21,23–25,28] The effect is due to a stiffening of the force field around the low-coordinated atoms, resulting from a shortening of the nearest-neighbor distances or a capillary pressure.

When turning to the lowest frequency $\omega_1(N)$, we see very strong size effects. For example, in going from Ni_{33} to Ni_{34}, the lowest frequency changes from 2.6 to 7×10^{12} s^{-1}. The geometric mean of the frequencies [important for classical thermodynamics in calculations of different thermodynamic potentials; see the short discussion following Eq. (2)], $\bar{\omega}(N) = \sqrt[N_v]{\prod_{i=1}^{N_v} \omega_i(N)}$ with N_v being the number of vibrational modes, shows a strong size dependence but without any important oscillations up to N around 30. For larger cluster sizes it is almost constant. Finally, Fig. 1 also shows, through the example $N = 38$, that the frequencies depend strongly on the structure type. The narrow panels of Fig. 1 display the full vibrational spectrum of the first (fcc structure, point group O_h) and the second-lowest (icosahedral structure, point group C_{5v}) isomers of Ni_{38} and Cu_{38}. As evident from the figures, the frequencies of the second, icosahedral isomers (for both nickel and copper), are shifted to larger values in accord with the structural considerations of the previous paragraph. However, it should be noted that the geometric mean frequency (that depends on the distribution of normal frequencies over the complete vibrational spectrum) for the first (fcc) isomer is larger than that for the icosahedral one: $\bar{\omega}(N) = 3.290 \times 10^{13}$ s^{-1} for $Ni_{38.1}$ and 3.283×10^{13} s^{-1} for $Ni_{38.2}$.

Once the vibrational properties have been determined, it is possible to determine further vibrational thermodynamic properties over a wide temperature range up to melting temperatures. Since for bulk copper the specific heat shows a deviation from the cubic temperature dependence that follows from the Debye phonon model only at a very low temperature of about 5 K, we assume for the metallic clusters of the present study that the electronic degrees of freedom can also be ignored when determining the thermodynamic properties. The approach used, based on statistical physics[44] and described further below, is to calculate the partition function Z and subsequently the Helmholtz free energy F, the entropy S, the inner energy E, and the heat capacity C. Thereby, we consider a canonical ensemble, which is similar to the experiments of the Haberland group.[37] Moreover, we use the harmonic superposition approximation[15,45,46] (SA) in the calculations of the thermodynamic properties. Furthermore, our treatment of the cluster thermodynamics is quantum mechanical. The main advantage of the SA method is that it is significantly faster than the more commonly used Monte Carlo approaches and it is ergodic. The high reliability of the harmonic SA for low-temperature thermodynamics of Lennard-Jones clusters was demonstrated expressively recently by two advanced Monte Carlo studies[47,48] using the improved replica exchange method. In the SA, the canonical partition function is written as a sum over contributions from all M significant minima of the potential energy surface (PES) as $Z(T) = \sum_{j=1}^{M} n_j Z_j(T)$ (T is the temperature), where Z_j is the partition function for minimum j. The term n_j is a degeneracy factor that takes into account the identical contributions from all the $2N!/o_j$ permutation-inversion isomers of structure j; o_j is the order of the point group, which is, for example, 114 for an icosahedron (I_h), 48 for a fcc structure (O_h), and 20 for a decahedron (D_{5h}). Furthermore, the probability P_{j1} of finding cluster structure $j1$ is given by $P_{j1}(T) = n_{j1} Z_{j1}(T) / \sum_{j=1}^{M} n_j Z_j(T)$.

First we present the results for a one-minimum model of the PES where only the global-minimum structures contribute to $Z(T)$. Our computations of different solid-solid transition temperatures have shown that for $T < 250$ K this approximation is good for the majority of Ni and Cu clusters from the cluster-size region $N = 2$–150. Then

$$
\begin{aligned}
Z &= \sum_n e^{-E_n/k_BT} = e^{-E_0/k_BT} \prod_{i=1}^{N_v} [2\sinh(\alpha_i/2)]^{-1}, \\
F &= -k_BT \ln Z = E_0 + k_BT \sum_{i=1}^{N_v} [\alpha_i/2 + \ln(1 - e^{-\alpha_i})], \\
S &= -\partial F/\partial T = k_B \sum_{i=1}^{N_v} [\alpha_i/(e^{\alpha_i} - 1) - \ln(1 - e^{-\alpha_i})], \quad (2) \\
E &= F + TS = \left(E_0 + \sum_{i=1}^{N_v} \hbar\omega_i/2 \right) + \sum_{i=1}^{N_v} \hbar\omega_i/(e^{-\alpha_i} - 1), \\
C &= \partial E/\partial(k_BT) = \sum_{i=1}^{N_v} \left[\alpha_i^2 e^{\alpha_i}/(e^{\alpha_i} - 1)^2 \right].
\end{aligned}
$$

In these equations, k_B is the Boltzmann constant and E_0 is the optimized total energy of a cluster at $T = 0$. Different $E_n = E_0 + \sum_{i=1}^{N_v} \hbar\omega_i(n_i + 1/2)$ with $n = \{n_1, n_2, \ldots, n_{N_v}\}$ are the different vibrational energy levels of the cluster; $\alpha_i = \hbar\omega_i/k_BT$. The formulas above include the zero-point contributions. Finally, the heat capacity is given in units of k_B. For $\alpha_i \ll 1$ (high temperatures), $2\sinh(\alpha_i/2) \approx \alpha_i$ and $Z = e^{-E_0/k_BT}/(\hbar\bar{\omega}/k_BT)^{3N-6}$. Thus, in a classical limit the partition function of an N-atomic cluster and, therefore, all the thermodynamic properties depend only on the geometric mean vibrational frequency $\bar{\omega}(N)$ and not the details of the vibrational spectrum of a cluster. Hence, in this case the geometric mean of normal-mode frequencies, which is of course a fictive mathematical magnitude, determines cluster vibrational thermodynamics.

At sufficiently elevated temperatures $k_BT \gg \hbar\omega_i$, C approaches the classical value of N_v. For very low temperatures

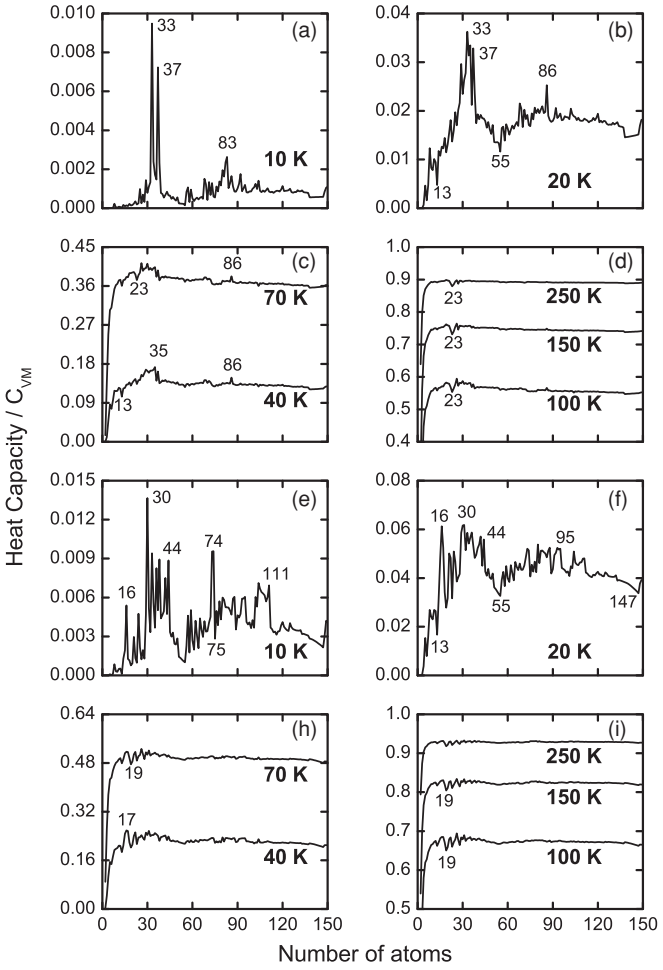

FIG. 2. Heat capacity of (a–d) Ni and (e–i) Cu clusters as a function of cluster size for different temperatures: (a, e) $T = 10$ K, (b, f) $T = 20$ K, (c, h) $T = 40$ and 70 K, and (d, i) $T = 100$, 150, and 250 K.

$k_BT \ll \hbar\omega_i$, C approaches $(\hbar\omega_1/k_BT)^2 \exp(-\hbar\omega_1/k_BT)$, which differs markedly from the bulk cubic (Debye) temperature dependence. Thus, the vibrational heat capacity in clusters approaches zero faster than in bulk with decreasing temperature.

Figure 2 shows the average heat capacity per vibrational mode, $C_{VM} = C/N_v$, for nickel [Figs. 2(a)–2(d)] and copper [Figs. 2(e)–2(i)] clusters for different temperatures. For the lowest temperatures, we see a very strong dependence on cluster size. Thus, Ni clusters with, e.g., 33, 37, and, to a lesser degree, 83 and 86 atoms and Cu clusters with $N = 16$, 30, 44, 74, 95, and 111 (clusters with either low-symmetrical structures with incomplete geometrical shells or decahedral/fcc structures) have very large heat capacities, whereas the particularly stable, magic-numbered icosahedral clusters with $N = 13$, 23, 55, and 147 show the most pronounced minima at low temperatures. Thus, in the temperature range of our study we can identify a correlation between the maxima of the vibrational energy of Fig. 1 and the minima of the heat capacity. This correspondence is mathematically clear for very low temperatures because of the factor $\exp(-\hbar\omega_1/k_BT)$ in the heat capacity formula at this limit. As Fig. 2 suggests, the size dependence of C_{VM} becomes less pronounced with increasing temperature. Here, clusters with less than roughly 30 atoms represent an exception. The heat capacity cluster-size effects remain important even at medium temperatures ~250 K for both nickel and copper clusters. In the mean, the heat capacity plots for copper clusters show stronger oscillations and larger values than those for Ni clusters. The temperature dependence of the heat capacity, within the one-minimum model of the PES, is monotonic and C_{VM} increases with increasing T, approaching the classical value of 1 for large T.

In our earlier structure optimizations,[9,10] we determined not only the energetically lowest structure but also the second- and third-lowest ones. We can, therefore, use the vibrational spectra of those to study, e.g., a solid-solid transition temperature within a two-minima model of the PES. Two minima, "1" and "2," with $E_0^{(1)} < E_0^{(2)}$ can represent, e.g., two competing structural types as a decahedron and an icosahedron or a truncated octahedron and an icosahedron. In the superposition approximation[15,45] and at the transition temperature $T_{ss}(1 \Leftrightarrow 2)$, the two probabilities to find cluster structures 1 and 2, P_1 and P_2, have to be equal. The corresponding equation for the transition temperature of the structural change from 1 to 2 is given by $P_1[T_{ss}(1 \Leftrightarrow 2)] = P_2[T_{ss}(1 \Leftrightarrow 2)]$ or $n_1 Z_1[T_{ss}(1 \Leftrightarrow 2)] = n_2 Z_2[T_{ss}(1 \Leftrightarrow 2)]$. Using this expression and the lowest-energy structures of Ni and Cu clusters together with their vibrational spectra, we have studied the structural changes from fcc to icosahedral structure in 38-atom Ni and Cu clusters as well as from decahedral ($Ni_{79.1}$) to fcc ($Ni_{79.2}$) and from fcc ($Cu_{79.1}$) to decahedral ($Cu_{79.2}$) structures. As transition temperatures, we found 482 K for $Ni_{38.1} \Leftrightarrow Ni_{38.2}$, 587 K for $Cu_{38.1} \Leftrightarrow Cu_{38.2}$, and 87 K for $Cu_{79.1} \Leftrightarrow Cu_{79.2}$. Furthermore, we found that, despite the small total-energy difference of 0.04 eV between the two lowest isomers of Ni_{79}, the structural transition between them does not take place up to melting temperatures. Finally, we examined the phase transition between the two lowest-energy isomers of Ni_{33} and Cu_{33}. The first isomers do not show any dominant morphology—icosahedral, decahedral, tetrahedral, or fcc.[9,10] The second isomers are polyicosahedral. Both isomers are low symmetric. As the computations have shown, the structural changes occur at 675 K for Ni and 231 K for Cu.

Temperature or entropy effects are the driving forces which permit solid-solid transitions or transitions to the structures with larger entropy. Within the two-minima model there are two main contributions to the entropy that might enable such transitions in clusters: (1) vibrational entropy, which in the quantum-mechanical case is defined through a factor $\prod_{i=1}^{N_v}[2\sinh(\alpha_i/2)]^{-1}$, and (2) configuration entropy, which is defined by the number of the permutation-inversion isomers. In turn, this number depends on the symmetry of the structure and is determined by the order of the point group of a minimum (factor o_j). This second term favors transitions from more symmetrical structures to less symmetrical ones. Of course, contributions (1) and (2) yield reasonable transition temperatures below the melting temperatures only if both structural minima under consideration are energetically close to each other. The interplay of the above factors can provide a very wide range of transition temperatures, as has been obtained in the current study. For example, the extremely low transition temperature of 87 K for the structural change

from fcc (Cu_{79_1}) to decahedral (Cu_{79_2}) structures results from (i) both first isomers of Cu_{79} being energetically extremely close to each other; the total-energy difference between them makes up only 0.02 eV. (ii) Vibrational entropy at $T = 87$ K is larger by a factor of 1.49 for the decahedral isomer, and finally (iii) the configuration entropy, which is defined by the ratio of 48 (O_h, fcc) to 4 (C_{2v}, decahedral), is greater for the decahedral structure by a factor of 12. Hence, all three reasons (i)–(iii) strongly favor the fcc-to-decahedral structural transition in Cu_{79}.

Next we want to check whether the suggested solid-solid transitions occur before melting. To do this requires the determination of the melting temperature of a cluster, which is generally a function of cluster size. The creation of a consistent melting theory of clusters is a very challenging problem and is not a purpose of the recent study. So we made the estimation of the cluster melting temperatures, using a formula from Ref. 49:

$$T_{\mathrm{mc}} = \frac{C_c}{C_b} T_{\mathrm{mb}}, \tag{3}$$

where T_{mc} and T_{mb} are the melting temperatures of the cluster and the bulk, accordingly, and C_c and C_b are the (average, for clusters) coordination numbers of the atoms in the cluster and in the bulk, correspondingly. The results for T_{mc} predicted by Eq. (3) were in good agreement with those obtained via molecular-dynamics simulations.[49] For the average coordination number in 33/38/79-atomic clusters, the values of 7.82, 7.58, and 8.51, respectively, were obtained in our earlier works.[9,10] With $C_b = 12$ for fcc metals and the bulk melting temperatures of 1728 K (Ni) and 1358 K (Cu), the following cluster melting temperatures have been derived: (i) 1126 and 1092 K for Ni_{33} and Ni_{38}, respectively, and (ii) 885, 858, and 963 K for Cu_{33}, Cu_{38}, and Cu_{79}, respectively. All the calculated cluster melting temperatures are higher than the corresponding solid-solid transition temperatures. Hence, the predicted solid transitions might happen before the cluster melting.

Solid-solid temperature structural transitions have been intensively studied in Lennard-Jones (LJ) and essentially less in Morse and metal clusters. Some selected references represent these studies: Refs. 47, 48, and 50 (LJ, and both Monte Carlo and SA approaches), Refs. 51–54 (Morse, LJ, Sutton-Chen, and Gupta potentials; SA approach), and Refs. 55–57 [EAM-like potentials (Ag, Au, Cu, Ni), molecular dynamics simulations, and the Monte Carlo method]. More studies on solid-solid transitions can be found in an excellent review article[41] and in recent studies.[47,48]

None of these studies considered structural changes from fcc to decahedral structure and vice versa, so we try to compare the obtained results for T_{ss} for only 33 and 38 clusters with previous calculations. However, such a comparison has to be done with care. Only one example illustrates that approach: phase diagrams for silver clusters derived in studies[52,54] using Sutton-Chen and Gupta potentials, respectively, are very different. None of the above studies use the EAM potential along with the SA. In a Monte Carlo study[56] by Vlachov *et al.*, part of the calculations were performed using the EAM potential. In particular, they could find that for Ni_{33} a structural change occurs at ~600 K (actually the transition temperature is between 600 and 700 K, as may be seen from Fig. 1 of Ref. 56), which is in good agreement with the temperature of 675 K derived in the present study. Furthermore, using the values of 0.5168 eV (Ni)[56] and 0.4093 eV (Cu)[58] for the parameter ϵ of the LJ potential and the dimensionless solid-solid transition temperature of 0.121 for LJ_{38} (Ref. 52) [$T_{\mathrm{ss}} = T_{\mathrm{ss}}^{\mathrm{LJ}}(\epsilon k_B^{-1})$], the transition temperatures of 726 and 575 K have been found for the 38-atom nickel and copper clusters within the LJ model. Good agreement between the EAM and LJ transition temperatures for Cu_{38} is surprising and rather accidental, whereas the significant disagreement for nickel clusters is understandable. That is because the many-body EAM potential describes the bonding in metal clusters more realistically than the simple pair (LJ) potential.[4] Furthermore, in an earlier study of Ni_N clusters ($N = 2$–150),[9] we found excellent agreement between the obtained EAM structures of nickel clusters and those from the chemical-probe experiments of Parks *et al.* (see references in Ref. 9). Next, in a molecular dynamics study,[57] Balleto *et al.* modeled the interatomic interaction in Cu_{38} and Ag_{38} via many-body Gupta potential. They found that in Cu_{38} the structural changes occur at intermediate temperatures of $300 < T < 450$ K, which are lower than those discussed above. Thus, for a consensus, more studies are needed.

In summary, we have determined the full vibrational spectrum of nickel and copper clusters with up to 150 atoms for the first time. Furthermore, using those spectra and the superposition approximation, we have calculated the thermodynamic properties of the clusters quantum mechanically, including their heat capacity and solid-solid transition temperatures for several structural changes in the Ni and Cu clusters. Both the vibrational spectrum and the thermodynamic functions show strong cluster-size effects. We emphasized that the approach used is general. It is based only on the (common) EAM form of the total energy [Eq. (1)] and is applicable to many other many-body potentials.

This work was supported by the Deutsche Forschungsgemeinschaft (DFG) through Project No. Sp439/23-1.

*Corresponding author : vg.grigoryan@mx.uni-saarland.de
†m.springborg@mx.uni-saarland.de

[1] M. S. Daw and M. I. Baskes, Phys. Rev. Lett. **50**, 1285 (1983).
[2] M. S. Daw and M. I. Baskes, Phys. Rev. B **29**, 6443 (1984).
[3] S. M. Foiles, M. I. Baskes, and M. S. Daw, Phys. Rev. B **33**, 7983 (1986).
[4] M. S. Daw, S. M. Foiles, and M. I. Baskes, Mater. Sci. Rep. **9**, 251 (1993).
[5] A. F. Voter and S. P. Chen, in *Characterization of Defects in Materials*, edited by R. W. Siegal, J. R. Weertman, and R. Sinclair, MRS Symposia Proceedings No. 82 (Materials Research Society, Pittsburgh, Pa, 1987), p. 175.
[6] A. F. Voter, in *Intermetallic Compounds*, edited by J. H. Westbrook and R. L. Fleischer (Wiley, New York, 1995), Vol. 1, p. 77.
[7] J. S. Nelson, E. C. Sowa, and M. S. Daw, Phys. Rev. Lett. **61**, 1977 (1988).

[8] J. S. Nelson, M. S. Daw, and E. C. Sowa, Phys. Rev. B **40**, 1465 (1989).
[9] V. G. Grigoryan and M. Springborg, Phys. Rev. B **70**, 205415 (2004).
[10] V. G. Grigoryan, D. Alamanova, and M. Springborg, Phys. Rev. B **73**, 115415 (2006).
[11] V. G. Grigoryan and M. Springborg, Phys. Chem. Chem. Phys. **3**, 5125 (2001).
[12] V. G. Grigoryan and M. Springborg, Chem. Phys. Lett. **375**, 219 (2003).
[13] V. G. Grigoryan, D. Alamanova, and M. Springborg, Eur. Phys. J. D **34**, 187 (2005).
[14] T. L. Hill, *Thermodynamics of Small Systems* (Dover, New York, 2002).
[15] D. J. Wales, *Energy Landscapes with Applications to Clusters, Biomolecules and Glasses* (Cambridge University, Cambridge, UK, 2003).
[16] A. Posada Amarillas and I. L. Garzón, Phys. Rev. B **54**, 10362 (1996).
[17] I. A. Solov'yov, A. V. Solov'yov, and W. Greiner, Phys. Rev. A **65**, 053203 (2002).
[18] A. Fielicke, A. Kirilyuk, C. Ratsch, J. Behler, M. Scheffler, G. von Helden, and G. Meijer, Phys. Rev. Lett. **93**, 023401 (2004).
[19] H. Yildrim, A. Kara, and T. S. Rahman, J. Phys. Condens. Matter **21**, 084220 (2009).
[20] A. Kara and T. S. Rahman, Phys. Rev. Lett. **81**, 1453 (1998).
[21] D. Y. Sun, X. G. Gong, and X.-Q. Wang, Phys. Rev. B **63**, 193412 (2001).
[22] X. Hu, G. Wang, W. Wu, P. Jiang, and J. Zi, J. Phys. Condens. Matter **13**, L835 (2001).
[23] R. Meyer, S. Prakash, and P. Entel, Phase Transitions **75**, 51 (2002).
[24] R. Meyer, L. J. Lewis, S. Prakash, and P. Entel, Phys. Rev. B **68**, 104303 (2003).
[25] A. Kara and T. S. Rahman, Surf. Sci. Rep. **56**, 159 (2005).
[26] A. Valentin, J. S'ee, S. Galdin-Retailleau, and P. Dollfus, J. Phys. Conf. Ser. **92**, 012048 (2007).
[27] B. Roldan Cuenya, A. Naitabdi, J. Croy, W. Sturhahn, J. Y. Zhao, E. E. Alp, R. Meyer, D. Sudfeld, E. Schuster, and W. Keune, Phys. Rev. B **76**, 195422 (2007).
[28] R. Meyer and D. Comtesse, Phys. Rev. B **83**, 014301 (2011).
[29] B. Fultz, J. L. Robertson, T. A. Stephens, L. J. Nagel, and S. Spooner, J. Appl. Phys. **79**, 8318 (1996).
[30] H. N. Frase, L. J. Nagel, J. L. Robertson, and B. Fultz, Philos. Mag. B **75**, 335 (1997).
[31] U. Stuhr, H. Wipf, K. H. Andersen, and H. Hahn, Phys. Rev. Lett. **81**, 1449 (1998).
[32] E. Bonetti, L. Pasquini, E. Sampaolesi, A. Deriu, and G. Cicognani, J. Appl. Phys. **88**, 4571 (2000).
[33] L. Pasquini, A. Barla, A. I. Chumakov, O. Leupold, R. Rüffer, A. Deriu, and E. Bonetti, Phys. Rev. B **66**, 073410 (2002).
[34] P. M. Derlet, R. Meyer, L. J. Lewis, U. Stuhr, and H. Van Swygenhoven, Phys. Rev. Lett. **87**, 205501 (2001).
[35] P. M. Derlet and H. V. Swygenhoven, Phys. Rev. Lett. **92**, 035505 (2004).
[36] M. Schmidt, R. Kusche, B. v. Issendorff, and H. Haberland, Nature (London) **393**, 238 (1998).
[37] M. Schmidt and H. Haberland, C. R. Phys. **3**, 327 (2002).
[38] H. Haberland, Th. Hippler, J. Donges, O. Kostko, M. Schmidt, and B. von Issendorff, Phys. Rev. Lett. **94**, 035701 (2005).
[39] A. A. Shvartsburg and M. F. Jarrold, Phys. Rev. Lett **85**, 2530 (2000).
[40] G. A. Breaux, R. C. Benirschke, T. Sugai, B. S. Kinnear, and M. F. Jarrold, Phys. Rev. Lett. **91**, 215508 (2003).
[41] F. Baletto and R. Ferrando, Rev. Mod. Phys. **77**, 371 (2005).
[42] F. Ahmed and E. R. Nixon, J. Chem. Phys. **71**, 3547 (1979).
[43] R. S. Ram, C. N. Jarman, and P. F. Bernath, J. Mol. Spectrosc. **156**, 468 (1992).
[44] L. D. Landau and E. M. Lifshitz, *Statistical Physics* (Pergamon, New York, 1980), Pt. 1.
[45] D. Wales, Mol. Phys. **78**, 151 (1993).
[46] J. P. K. Doye and D. Wales, J. Chem. Phys. **102**, 9659 (1995).
[47] V. A. Sharapov, D. Meluzzi, and V. A. Mandelshtam, Phys. Rev. Lett. **98**, 105701 (2007).
[48] V. A. Sharapov and V. A. Mandelshtam, J. Phys. Chem. A **111**, 10284 (2007).
[49] C. Rey, L. J. Gallego, J. García-Rodeja, J. A. Alonso, and M. P. Iñiguez, Phys. Rev. B **48**, 8253 (1993).
[50] G. Adjanor, M. Athènes, and F. Calvo, Eur. Phys. J. B **53**, 47 (2006).
[51] J. P. K. Doye, D. Wales, and F. Calvo, J. Chem. Phys. **103**, 4234 (1995).
[52] J. P. K. Doye and F. Calvo, Phys. Rev. Lett. **86**, 3570 (2001).
[53] J. P. K. Doye and F. Calvo, J. Chem. Phys. **116**, 8307 (2002).
[54] F. Calvo and J. P. K. Doye, Phys. Rev. B **69**, 125414 (2004).
[55] C. L. Cleveland, W. D. Luedtke, and U. Landman, Phys. Rev. Lett. **81**, 2036 (1998); Phys. Rev. B **60**, 5065 (1999).
[56] D. G. Vlachos, L. D. Schmidt, and R. Aris, J. Chem. Phys. **96**, 6891 (1992).
[57] F. Baletto, A. Rapallo, G. Rossi, and R. Ferrando, Phys. Rev. B **69**, 235421 (2004).
[58] J. Yu and J. G. Amar, Phys. Rev. Lett. **89**, 286103 (2002).